P2.21

# A Prototype Benchmark Thermal Radiance Measurement

John A. Dykema, James G. Anderson and R.M. Goody
Harvard University, Divsion of Engineering and Applied Sciences, Cambridge MA

## 1. Introduction

The NOAA Science Advisory Board's Panel on Strategies for Climate Monitoring prioritizes the development of a set of Benchmark measurements for monitoring long-term changes in climate. As defined by the Panel, Benchmark measurements adhere to principles requiring demonstrable accuracy tied to metrological standards on a limited set of climate variables relevant to decadal-to-century scale climate change. An illustrative example of a Benchmark measurement is the baseline $CO_2$ monitoring effort maintained by CMDL. Spectrally resolved, thermal radiance measurements from space constitute a key Benchmark measurement that is well-studied (Harries *et al.* 2001) and capable of early deployment. The realization of this benchmark measurement requires scientific infrastructure which is singularly focused on the radiometric accuracy target. This infrastructure connects precision measurements in the laboratory through identical hardware to on-orbit diagnostics in the satellite.

We present a numerical model which quantifies the expected radiometric performance of a prototype instrument for a benchmark radiance measurement. The model calculates the systematic error as a function of observed brightness temperature and wavenumber. The model is based on a design for a low-cost, lightweight satellite. This design includes two bore-sighted Michelson interferometers covering the spectral window from 250 to 2000 $cm^{-1}$ (40 to 5 μm) at a spectral resolution of ~ 0.5 $cm^{-1}$, with an accuracy goal of 0.1 K on at 250 K brightness temperature at 750 $cm^{-1}$. This level of accuracy in a space-based measurement represents a significant challenge. Because the satellite must satisfy the objective of convincing future investigators of accuracy, radiometric performance must be clearly documented.

The calibration strategy for this Benchmark measurement is based on the principles of precision metrology (Keith and Anderson 2001). Every source of systematic error that is significant at the 10 mK level will be measured independently. The end-to-end performance of the instrument will then be carefully quantified, and analyzed for its agreement with the constituent error sources. The model under development presented here provides a quantitative simulation of these systematic errors. The model is designed to both simulate the errors independently and calculate their effect as they would occur together in the real instrument. The parameters utilized by the model reflect the actual performance of instrumental subsystems as determined both by emipirical measurements and from engineering specifications. The model converts the subsytem parameters into their associated systematic radiometric errors, expressed in units of equivalent temperature. Errors related to the calibration standards (blackbodies) and instrumental optical performance are treated, including blackbody thermometry and emissivity, out of field of view optical sensitivity, infrared detector and signal chain nonlinearity, and polarization effects. These errors have been treated for other infrared radiometers (Fennelly *et al.* 2001, Best *et al*. 1997, Mason *et al*. 1996). The following table shows the design values for the individual errors simulated in this model (Anderson *et al*. 1995).

| Systematic Error | Value |
|---|---|
| Absolute Thermometry | 0.030 K |
| Blackbody Inhomogeneity | 0.035 K |
| Blackbody Emissivty | 0.9997 |
| Polarization Error | 0.0011*scene temperature contrast |
| Out-of-Field of View (FOV) Sensitivity | 0.01% |
| Signal Chain Nonlinearity | 0.0001 |

These errors are treated with the goal of providing a performance baseline for critical analysis of on-orbit accuracy and to evaluate effects of the space environment on the measurement calibration.

## 2. Numerical Model

A calibrating, spectrally resolving radiometer requires three basic components: calibration standards, a means of spectral dispersion, and a radiation detector. The candidate radiometer simulated by this model has three calibration standards: two blackbody cavities and a deep space view, to allow overdetermination of the calibration (assuming the radiometer has a linear response to incident flux). The level of measurement accuracy achieved during flight can therefore be critically analyzed by intercomparing the three calibration standards.

The blackbodies are composed of deep cylindrical cavities coated with very low reflectivity coating, which yields emissivity very near (but not perfectly) unity. The cavities are maintained at a stable temperature by closed loop control, monitored by redundant temperature sensors. For accurate determination of radiometric zero, a deep space view is included as a calibration standard. The systematic errors due to the blackbodies are related

Corresponding author address: John A. Dykema, Anderson Group/CCB, Harvard University, 12 Oxford St., Cambridge, MA 02138; e-mail: dykema@fas.harvard.edu

to differences between the true photon flux provided by the blackbody and the estimated photon flux from the measured thermometric temperature and the estimated emissivity.

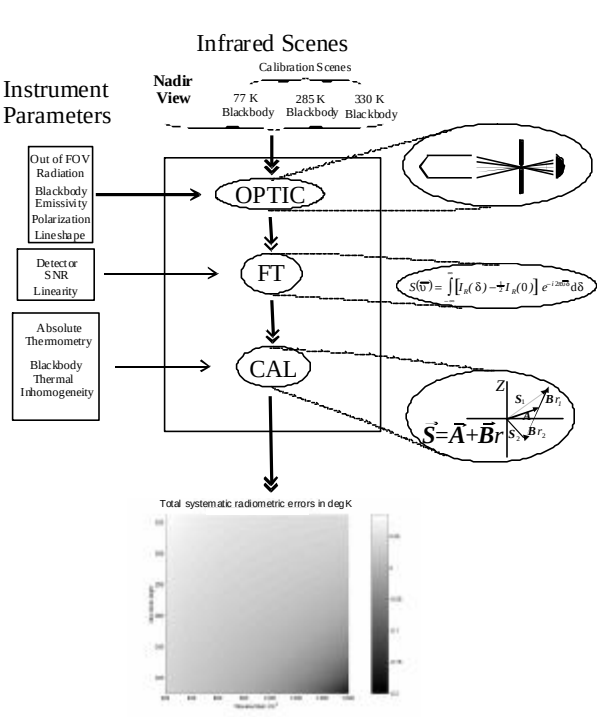


**Figure 1:** A flow chart of the numerical model of the prototype Benchmark spectrometer. Radiation scenes undergo sequential operations simulating the systematic errors specified by the characteristics of the actual instrumental hardware. The large central rectangle represents the numerical model; the left hand column represents the instrument subsystem parameters, which determine the magnitude of the systematic errors. The ellipses on the right hand side represent the internal calculations of the model. An observed scene plus two calibration scenes are processed from top to bottom, finally producing a calibrated output scene, from which the systematic errors are determined, as shown in the bottom plot.

A corner cube, four port FTS provides spectral dispersion. The input port that views the scene (either calibration scene or atmospheric scene) is differenced against a stable radiometric standard. An optical pointing system is required to select the light that is directed into this input port. This action is accomplished via a pointing mirror. The systematic errors due to the spectral disperser and optical system are related to stray light which is directed into the observation scene, and to changes in optical efficiency due to polarization effects as the pointing mirror rotates relative to the FTS beamsplitter.

At each detector port, a pyroelectric detector senses the interferometric signal. Although pyroelectric detectors have relatively low detectivity (D*) and thus lower signal-to-noise ratio (SNR) than quantum detectors such as mercury cadmium telluride (MCT) detectors, they have a much more linear response and cover a wider spectral window with nearly constant responsivity. The systematic errors associated with the detector are due to nonlinearities in its response and within the signal chain. The noise intrinsic to the detector (as measured by D*) adds a random noise component to the spectral measurement.

As shown in figure 1, the model performs sequential operations that simulate the changes to the observed radiation field due to the characteristics of the instrument. To calculate the error for a given observation scene, three spectral acquisitions are simulated: the observation scene itself, and two calibration scenes. The calibration scenes are necessary to derive the calibration coefficients as per Revercomb *et al* (1988).

The first module of the model simulates the optical properties of the spectrometer. For blackbody calibration scenes, the radiance is calculated from the planck function for the chosen calibration temperature. Calibration temperatures are chosen to bracket the expected range of observation temperatures, which are expected to be between 180 K and 320 K. This radiance is then multiplied by a factor less than one to simulate the imperfect emissivity of the blackbody cavity.

$$r_{bb} = e\, r_{planck}(T)$$

Here a constant value of ε for all wavenumbers is used, although a factor which is a function of wavenumber may be used if detailed measurements show significant frequency-dependent emissivity. The value of ε used for this work was 0.9997. This emissivity may be readily achieved by utilizing Enhanced Martin Black coating in a cavity with a diameter to aperture ratio of 3.

The next step is to simulate stray radiation which is modulated by the interferometer and enters the infrared detector. (Laboratory observations indicate radiation from outside the field of view is well approximated by thermal radiation at ambient instrument temperature). The observed radiation is modeled as a linear combination of the scene radiation from the previous operation and blackbody radiation at the temperature of the instrument optics.

$$r_{scene} = (1-b)\, r_{scene} + b\; r_{ambient}(t,T)$$

The value of the out of field sensitivity $b$ used for this work was 0.01%. Because this ambient radiation represents an offset to the scene radiance, the calibration procedure will compensate for it if it is stable over an acquisition cycle. If it varies between acquisitions of calibration and observation scenes, an error will be introduced. To simulate this property, the model varies the temperature of the ambient radiation and the reference input between data acquisitions. This introduces the thermal stability of the instrument as a significant source of systematic error. The thermal stability of the reference input was 400 min/K. The thermal stability of the emission temperature of the ambient (stray) radiation was 80 min/K.

The next step simulates the polarization effect due to changes in orientation between the optical axes of the pointing mirror and the beamsplitter. The reflectivity of the pointing mirror is slightly different for radiation polarized parallel and perpendicular to the plane of reflection (called s- and p-reflectivities). The correction takes the form:

$$r_{pol} = r\cos(2q)(r_{scene} - r_{PM}) + r_{scene}$$

where $r_{pol}$ is the scene radiation transformed by the polarization effect, $r$ is a parameter measured empirically or derived from the known optical properties of the pointing mirror and beamsplittter $q$ is the angle between the plane of reflection at the pointing mirror and the optical axes of the beamsplitter, and $r_{scene}$ is the scene radiation from the previous model step. The value for $r$ here is 0.0011, taken from measurements on INTESA (Keith *et al* 2001). This value creates a radiometric error of about one part per thousand in the mid-infrared. This error may be measured by viewing a fixed scene over a range of pointing mirror angles. This procedure can be accomplished in a satellite by viewing deep space over a range for 45°, producing a value for $r$. This value can then be used with the above equation to correct the measured radiance.

As stated above, the spectrometer model is based on a four-port interferometer with two input ports and two output ports. A radiometric reference is placed at the second input port (the first being dedicated to scene radiation selected by the pointing mirror). The radiation detected at the interferometer output ports is then a difference spectrum created by the difference of the scene radiation and the reference radiation. This characteristic is simulated by subtracting blackbody radiance for the temperature of the reference input (typically 5 K below ambient temperature) from the scene radiation.

This difference spectrum is next converted into an interferogram by an inverse Fourier transform. A nonlinear response in the detector signal chain may be approximated by a power series in the interferogram (Abrams *et al.* 1994). For the small nonlinearities required for this spectrometer, inclusion of a quadratic term is sufficient. The interferogram is thus transformed:

$$I_{nl} = I_{obs} + aI_{obs}^2$$

Since the candidate detector for this spectrometer is pyroelectric, the interferogram consists only of an AC modulated signal. Pyroelectric detectors only detect time-changing signals (Porter 1981). The nonlinearity in this model reduces the centerburst magnitude of the brightest scene by 0.01%.

Quantum photodetectors which are sensitive to DC background radiation require an offset term:

$$I_{nl} = (I_{obs} + \Phi_{DC}) + a(I_{obs} + \Phi_{DC})^2$$

This DC flux creates an additional radiometric error which is proportional to the scene radiance.

After the nonlinearity is simulated, the scene is returned to spectral form via a Fourier transform. The radiometric error on the scene may now be calculated by following the calibration procedure, which incorporates errors due to absolute thermometry and blackbody thermal inhomogeneity.

The systematic errors associated with this module arise due to differences between the predicted blackbody radiation flux and actual blackbody radiation flux that are constant in equivalent temperature. These errors arise from temperature gradients in the blackbody cavity, temperature differences between the location of the temperature sensor and the emitting surface, and from inaccuracies in measurement by the temperature sensors themselves.

The calibration coefficients are calculated by solving the system of equations:

$$S_{i,\tilde{n}} = A_{i,\tilde{n}} + B_{i,\tilde{n}} r_{i,\tilde{n}}$$

where $S$ is the observed radiance signal for each blackbody $i$ and channel $\tilde{n}$, and $r$ is the true radiance calculated from the Planck function. $A$ and $B$ are the calibration coefficients, computed for each wavenumber channel. $A$ represents the optical offset vector, $B$ represents the instrument gain. The thermometry errors are simulated by computing a blackbody radiance $r$ for a temperature differing from the blackbody scene temperature by some error $dT$.

$$r_{i,\tilde{n}} = r_{planck}(T - dT)$$

The value for the thermometry error $dT$ used for this work is 0.065 K. This value includes 0.03 K absolute thermometry error (inaccuracy of the temperature sensor) plus 0.035 K blackbody inhomogeneity error (spatial temperature inhomogeneity of the blackbody, difference between temperature of emitting surface and region of temperature sensor).

## Results

The calculation of the radiometric error in equivalent temperature units was performed for brightness temperatures ranging from 210 K to 325 K, for frequencies from 200 $cm^{-1}$ to 1600 $cm^{-1}$. The results for these calculations are shown in figure 2. This figure shows that the highest levels of accuracy are achieved in the middle of the instrument's spectral window, between 500 $cm^{-1}$ and 1000 $cm^{-1}$. This spectral region covers several important radiative forcings, including $CO_2$, CFC-11 and CFC-12 and $O_3$. CH4 and water vapor have strong radiative forcings nearby between 1100-1300 $cm^{-1}$, where radiometric accuracy is also good except for very cold equivalent temperatures.

The errors at warm temperatures are dominated by the nonzero reflectivity of the blackbodies. This effect produces a warm bias on the measurement, which is most pronounced for the hottest scenes and is near zero for very cold scenes. At cold temperatures, the errors are dominated by stray light effects, which are largest at higher frequencies. Because cold scenes emit a relatively low quantity of radiation at these frequencies, stray radiation from warm scenes has an exaggerated effect. The nonlinearity errors are most pronounced at the edges of the spectral window, where the ratio of aliased radiance to real radiance is largest. Thermometry errors create a radiometric error that is nearly equal in equivalent temperature across the window. Polarization errors are largest for scenes that are either very hot or very cold, since they are proportional to the temperature contrast between the pointing mirror and the scene.

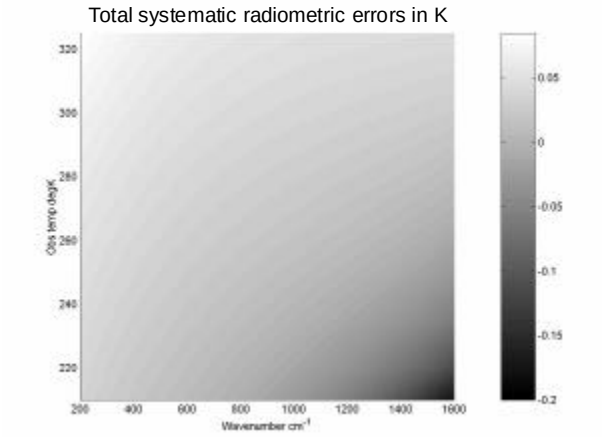


**Figure 2** Results of model calculation for error budget given in table 1. The calculations predict that the instrument will demonstrate better than 0.1 K radiometric accuracy for frequencies between 500-1000 $cm^{-1}$ for all brightness temperatures between 210-325 K. Between 1100-1400 $cm^{-1}$, better than 0.1 K accuracy is achieved for brightness temperatures above 240 K. This performance meets the requirements for monitoring the decadal-scale trends in the radiative forcing due to the key greenhouse gases $CO_2$, $CH_4$, $H_2O$, $N_2O$, $O_3$, CFC-11, and CFC-12.

## Conclusions

The radiometric performance of a prototype spectroradiometer for long-term climate monitoring may be simulated by a set of simple calculations that utilize parameters from engineering specifications and laboratory experiments. These calculations reveal significant spectral variation in the achieved radiometric accuracy, which also depends considerably on scene temperature. These results may be used as a tool to optimize instrumental design to efficiently monitor long-term changes in climate.

## References

Abrams, M. C., Toon, G. C., Schindler, R. A., 1994: Practical example of the correction of Fourier-transform spectra for detector nonlinearity. *Applied Optics*, **33**, 6307-6314.

Anderson, J. G., Keith, D. W., Goody, R.G., and Coauthors, 1996: Arrhenius: A small satellite for climate research. A proposal submitted to NASA-HQ December 1996, No. ESSP-II-0030, 160 pp. [Available from the authors]

Best, F., H. Revercomb, D. LaPorte, R. Knuteson, and W. Smith, Accurately Calibrated Airborne and Ground-based Fourier Transform Spectrometers II:HIS and AERI Calibration Techniques, Traceability, and Testing, in *Council for Optical Radiation Measurements (CORM) 1997 Annual Meeting*, National Institute of Standards and Technology (NIST), Gaithersburg, MD, 1997.

Fennelly, J., J.E. Jenney, D. Jordan, and P. Mantica, Challenges in calibration of operation fourier transform spectrometers for space-based nadir sounding of the earth's atmosphere, in *Fourier Transform Spectroscopy And Optical Remote Sensing of the Atmosphere*, Optical Society of America, Couer d'Alene, ID, 2001.

Harries, J.E., H.E. Brindley, P.J. Sagoo, and R.J. Bantges, Increases in greenhouse forcing inferred from the outgoing longwave radiation spectra of the Earth in 1970 and 1997, *Nature*, *410*, 355-357, 2001.

Keith, D. W., and Anderson, J.G., 2001: Accurate Spectrally Resolved Infrared Radiance Observation from Space: Implications for the Detection of Decade-to-Century–Scale Climatic Change, *Journal of Climate,* **14**, 979–990.

Keith, D.W., J.A. Dykema, H. Hu, L. Lapson, and J.G. Anderson, An Airborne Interferometer for Atmospheric Emission and Solar Absorption, *Applied Optics*, in press

Mason, I.M., P.H. Sheather, J.A. Bowles, and G. Davies, Blackbody calibration sources of high accuracy for a spaceborne infrared instrument: The Along Track Scanning Radiometer, *Applied Optics*, *35* (4), 629-639, 1996.

Porter, S.G., A brief guide to pyroelectric detectors, *Ferroelectrics*, *33* (1-4), 193-206, 1981.

Revercomb, H.E., H. Buijs, H.B. Howell, D.D. Laporte, W.L. Smith, and L.A. Sromovsky, 1988: Radiometric calibration of IR Fourier-transform spectrometers - solution to a problem with the high-resolution interferometer sounder, *Appied Opt*ics, **27**, 3210-3218.